



ARL-TN-1204 • JUNE 2024



Mechanical Properties of Additively Manufactured AlSi10Mg with Respect to Build Orientation

by Alex Butler, Brandon McWilliams, and Josh Taggart-Scarff

NOTICES

Disclaimers

The findings in this report are not to be construed as an official Department of the Army position unless so designated by other authorized documents.

Citation of manufacturer's or trade names does not constitute an official endorsement or approval of the use thereof.

Destroy this report when it is no longer needed. Do not return it to the originator.



Mechanical Properties of Additively Manufactured AlSi10Mg with Respect to Build Orientation

Alex Butler and Brandon McWilliams
DEVCOM Army Research Laboratory

Josh Taggart-Scarff
SURVICE Engineering

REPORT DOCUMENTATION PAGE

1. REPORT DATE		2. REPORT TYPE		3. DATES COVERED	
June 2024		Technical Note		START DATE 12/8/2023	END DATE 5/1/2024
4. TITLE AND SUBTITLE Mechanical Properties of Additively Manufactured AlSi10Mg with Respect to Build Orientation					
5a. CONTRACT NUMBER		5b. GRANT NUMBER		5c. PROGRAM ELEMENT NUMBER	
5d. PROJECT NUMBER		5e. TASK NUMBER		5f. WORK UNIT NUMBER	
6. AUTHOR(S) Alex Butler, Brandon McWilliams, and Josh Taggart-Scarff					
7. PERFORMING ORGANIZATION NAME(S) AND ADDRESS(ES) DEVCOM Army Research Laboratory ATTN: FCDD-RLA-MD Aberdeen Proving Ground, MD 21005				8. PERFORMING ORGANIZATION REPORT NUMBER ARL-TN-1204	
9. SPONSORING/MONITORING AGENCY NAME(S) AND ADDRESS(ES)		10. SPONSOR/MONITOR'S ACRONYM(S)		11. SPONSOR/MONITOR'S REPORT NUMBER(S)	
12. DISTRIBUTION/AVAILABILITY STATEMENT DISTRIBUTION STATEMENT A. Approved for public release: distribution unlimited.					
13. SUPPLEMENTARY NOTES ORCIDs: Alex Butler, 0009-0002-3705-4961; Brandon McWilliams, 0000-0002-0494-3140; Josh Taggart-Scarff, 0000-0003-3540-7436					
14. ABSTRACT Anisotropic material properties are common in additively manufactured metals due to the directional nature of the manufacturing process. Understanding the impact of mechanical properties with respect to build direction allows researchers and engineers to make informed decisions regarding part design and build orientation. These decisions can influence part performance and confidence, especially in critical applications. This work found that for additively manufactured AlSi10Mg using laser-powder bed fusion, the direction perpendicular to the direction of printing (horizontal) shows a 2% decrease in ultimate tensile strength compared to the direction aligned with the print direction (vertical); however, the strain at failure, elastic modulus, and yield stress increased by 53%, 15%, and 8%, respectively.					
15. SUBJECT TERMS Sciences of Extreme Materials, additive manufacturing, AlSi10Mg, laser-powder bed fusion, process optimization					
16. SECURITY CLASSIFICATION OF:				17. LIMITATION OF ABSTRACT UU	18. NUMBER OF PAGES 20
a. REPORT UNCLASSIFIED	b. ABSTRACT UNCLASSIFIED	c. THIS PAGE UNCLASSIFIED			
19a. NAME OF RESPONSIBLE PERSON Alex Butler				19b. PHONE NUMBER (410) 306-0751	

STANDARD FORM 298 (REV. 5/2020)
Prescribed by ANSI Std. Z39.18

Contents

List of Figures	iv
List of Tables	iv
1. Introduction	1
2. Experimental	1
2.1 Feedstock	1
2.2 Samples	2
2.3 Mechanical Testing	3
4. Results	4
5. Conclusion	9
6. References	10
Appendix. Mechanical Testing Results	11
List of Symbols, Abbreviations, and Acronyms	14

List of Figures

Fig. 1	Sieved AlSi10Mg particle-size distribution.....	2
Fig. 2	STL files of tensile bar stacks in the vertical, horizontal, and 45° directions.....	3
Fig. 3	Stress-strain curves for tensile samples printed in different build orientations.....	6
Fig. 4	2D and 3D micrographs of fracture surface of tensile samples	8
Fig. A-1	Tensile testing results with lines denoting which samples were statistically similar	12
Fig. A-2	Impact testing results	13

List of Tables

Table 1	Elemental composition of AlSi10Mg aluminum powder feedstock.....	2
Table 2	EOS M290 AlSi10Mg build parameters.....	3
Table 3	ANOVA analysis results.....	5
Table 4	Results of Tukey's test.....	6
Table 5	Mechanical properties for different build orientations	7
Table 6	Percentage changes in mechanical responses compared to the vertical direction with bolded values showing no statistical difference between samples.....	7

1. Introduction

Additive manufacturing (AM) processes provide increased design flexibility and reduced lead times. However, these layer-wise processes have their own design challenges that must be understood to use the technology to its full potential. Laser-powder bed fusion (LPBF) is an AM process in which powder is spread over a build plate using a recoater mechanism and then a laser selectively melts the powder. The build plate lowers, another layer of powder is spread, and the process repeats, yielding a fully dense part attached to the build plate, surrounded by loose powder.

The directionality of this process can yield anisotropic properties. The layer-wise process, which includes subjecting previous layers to intense heat as the layers above are being deposited, yields unique thermal histories. These thermal histories can lead to microstructural changes, internal stresses, and defect formation.

When setting up the build for the LPBF process, orientation of the part is crucial to avoid overhangs (features with a downward face). These features lead to increased surface roughness and, at severe angles, build failure. The overhangs can be mitigated by introducing support material, which acts like a scaffolding to deposit on top. However, removal of these support materials can require additional post-processing steps, such as machining or using hand tools. An understanding of the response of the printed material to build orientation can better inform users when orienting parts for AM, increasing build confidence and part performance.

2. Experimental

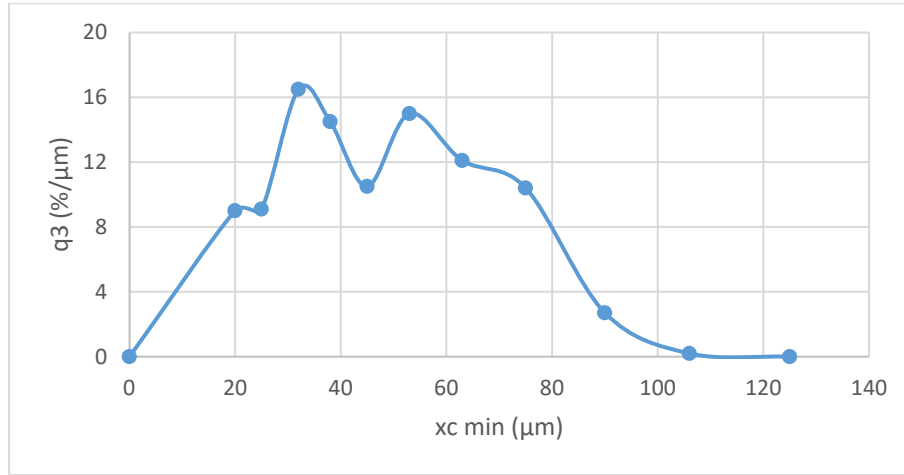
To characterize the mechanical properties of different print orientations, testing was conducted to evaluate the performance of the material. The results were then analyzed using analysis of variance (ANOVA) and Tukey's post hoc analysis to identify statistically dissimilar results. A description of the manufacture and testing of the samples is provided.

2.1 Feedstock

Aluminum, silicon, magnesium alloy (AlSi10Mg) powder was used as the feedstock for the samples. The composition of the powder is shown in Table 1. The powder was reused and sieved in between builds using a 90- μ m mesh screen. The particle-size distribution of the powder was recorded via dynamic image analysis on the CAMSIZER X2 (Fig. 1).

Table 1 Elemental composition of AlSi10Mg aluminum powder feedstock

Composition weight percentage										
Si	Fe	Cu	Mn	Mg	Ni	Zn	Pd	Sn	Ti	Al
10.0	≤0.55	≤0.05	≤0.45	0.33	≤0.05	≤0.10	≤0.05	≤0.05	≤0.15	Balance

**Fig. 1** Sieved AlSi10Mg particle-size distribution

2.2 Samples

Tensile (ASTM E8¹) and Charpy (ASTM E23²) V-notch impact samples were manufactured on the EOS M290 LPBF system. The processing parameters in Table 2 were built under argon with a stainless steel recoater blade. Note that these are the Original Equipment Manufacturer (OEM)’s (EOS) default parameters for AlSi10Mg as of 2023. Both types of mechanical test samples were printed in two orientations to quantify material anisotropy. A set of coupons was produced with the loading axis perpendicular to the axis of printing, which will be referred to as “horizontal,” and a set of coupons was produced with the loading axis aligned with the printing direction, which will be referred to as “vertical.” In addition, tensile samples were printed at a 45° angle with respect to the build platform. The tensile samples were initially printed in larger blocks, which resembled E8 subsize tensile bars (Fig. 2). Using wire electrical discharge machining, the parts were removed from the build plate, tensile bars were sliced from the larger blocks, and the Charpy bars were notched. All samples were machined to final dimensions in accordance with ASTM standards.

Table 2 EOS M290 AlSi10Mg build parameters

Laser power (W)	Laser scan speed (m/s)	Hatch spacing (μm)	Layer thickness (μm)	Build plate temperature ($^{\circ}\text{C}$)
370	1.3	130	30	30

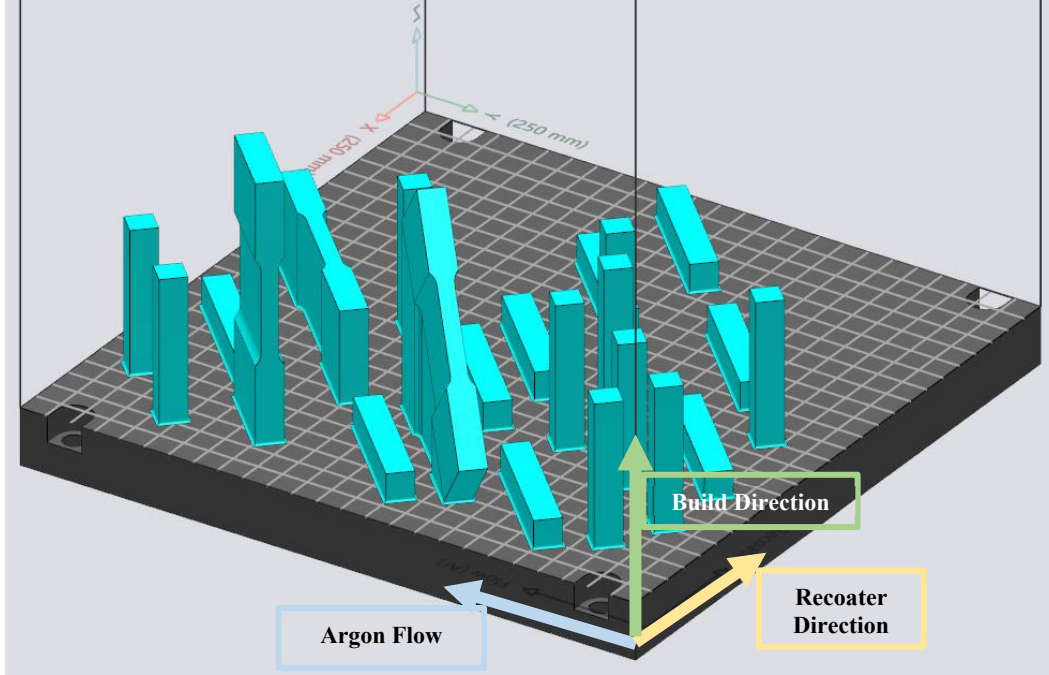


Fig. 2 STL files of tensile bar stacks in the vertical, horizontal, and 45° directions

2.3 Mechanical Testing

Following the procedures in ASTM E8/E8M,¹ the tensile samples were tested on the Instron 5984 electrical mechanical test frame at a constant displacement rate of 1.2 mm/min. The samples were painted white and speckled with black paint, and the cross-sectional dimension was measured before tensile testing. The 3D digital image correlation was used to obtain strain data. The 2D and 3D micrographs of the fracture surface were taken on the Keyence VHX7000. The area of fracture surface was measured to calculate the cross-sectional area reduction at failure. The Charpy samples were tested at room temperature, following the guidelines in ASTM E23-16b,² on a Tinius Olsen pendulum tester with a maximum energy capacity of 300 ft-lb.

4. Results

A one-way ANOVA ($\alpha = 0.05$) was performed to compare the results of each measured mechanical property for each build direction. The F value was compared to the F critical value. If the F value was greater than the F critical value, there was some statistical difference in the data. The analysis showed that for each mechanical property, there was a statistically significant difference between at least two orientations (Table 3). Tukey's post hoc test was used to identify which samples were statistically different from each other. The results of this test are reported in Table 4. Tukey's test showed that in all cases, the performance of the horizontal and vertical samples was significantly different. There were cases in which either or both the horizontal and vertical samples were not significantly different from the 45° samples.

Table 3 ANOVA analysis results

Ultimate tensile strength (UTS)						
Groups	Count	Sum	Average	Variance		
Horizontal	5	2149	429.9	2.23		
Vertical	4	1752	438.0	14.33		
45°	5	2187	437.4	15.16		
Source of variation	SS	df	MS	F	p value	F crit
Between groups	195.8	2	97.90	9.57	0.003917	3.98
Within groups	112.6	11	10.23
Total	308.4	13
Strain at failure						
Groups	Count	Sum	Average	Variance		
Horizontal	5	0.4505	0.0901	2.5E-05		
Vertical	4	0.235	0.05875	1.8E-05		
45°	5	0.3593	0.07186	2.11E-05		
Source of variation	SS	df	MS	F	p value	F crit
Between groups	0.002244	2	0.001122	51.75	2.54E-06	3.98
Within groups	0.000238	11	2.17E-05
Total	0.002482	13
Elastic modulus						
Groups	Count	Sum	Average	Variance		
Horizontal	5	332.0	66.41	0.69157		
Vertical	4	231.5	57.87	16.52		
45°	5	335.7	67.15	1.14		
Source of Variation	SS	df	MS	F	p value	F crit
Between groups	228.3	2	114.1	22.07	0.000141	3.98
Within groups	56.88	11	5.17
Total	285.2	13
Yield stress						
Groups	Count	Sum	Average	Variance		
Horizontal	5	1258	251.7	0.69205		
Vertical	4	929.3	232.3	36.11		
45°	5	1229	245.8	3.10		
Source of Variation	SS	df	MS	F	p value	F crit
Between groups	855.5	2	427.7	38.10	1.14E-05	3.98
Within groups	123.5	11	11.23
Total	979.0	13
Tensile area reduction						
Groups	Count	Sum	Average	Variance		
Horizontal	5	51	10.20	1.70		
Vertical	4	30	7.50	3.50		
45°	5	40	8	0.625		
Source of Variation	SS	df	MS	F	p value	F crit
Between groups	19.41	2	9.71	5.39	0.023319	3.98
Within groups	19.80	11	1.8
Total	39.21	13
Room temperature impact energy						
Groups	Count	Sum	Average	Variance		
Horizontal	10	60.79	6.08	0.006869		
Vertical	10	37.59	3.76	0.00751		
Source of Variation	SS	df	MS	F	p value	F crit
Between groups	26.91	1	26.91	3744	2.45E-22	4.41
Within groups	0.129409	18	0.007189
Total	27.04	19

Table 4 Results of Tukey's test

Performance metrics	Comparison	Absolute difference in means	$q_{crit}\sqrt{MS_w/n}$	Are they significantly different?
UTS	H to V	8.118	6.110	Yes
	H to 45	7.526	6.110	Yes
	V to 45	0.5925	6.110	No
Strain at failure	H to V	0.0314	0.0089	Yes
	H to 45	0.0182	0.0089	Yes
	V to 45	0.0131	0.0089	Yes
Elastic modulus	H to V	8.543	4.343	Yes
	H to 45	0.738	4.343	No
	V to 45	9.281	4.343	Yes
Yield strength	H to V	19.35	6.400	Yes
	H to 45	5.888	6.400	No
	V to 45	13.46	6.400	Yes
Tensile area reduction	H to V	2.7	2.563	Yes
	H to 45	2.2	2.563	No
	V to 45	0.5	2.563	No

Figure 3 shows the tensile stress-strain curves. The mechanical properties from tensile and impact testing are reported in Table 5, and percentage changes in performance from the vertical direction other build directions are reported in Table 6. Micrographs of the tensile sample fracture surfaces are shown in Fig. 4.

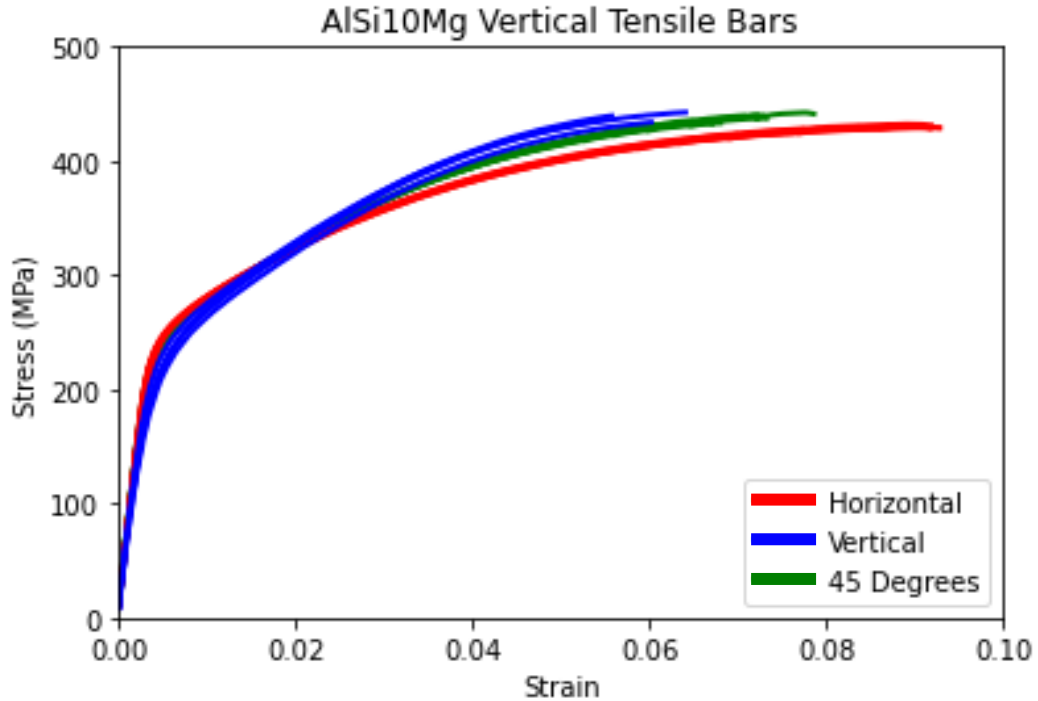
**Fig. 3 Stress-strain curves for tensile samples printed in different build orientations**

Table 5 Mechanical properties for different build orientations

Orientation	UTS (MPa)	Yield strength (MPa)	Elastic modulus (GPa)	Elongation (%)	Area reduction (%)	Room temperature impact energy (ft-lb)
Vertical	438.0 ± 3.8	232.3 ± 6.0	57.87 ± 4.06	5.88 ± 0.42	7.6 ± 1.76	3.75 ± 0.08
Horizontal	429.9 ± 1.5	251.7 ± 0.8	66.41 ± 0.83	9.01 ± 0.50	10.3 ± 1.1	6.08 ± 0.08
45°	437.4 ± 3.9	245.8 ± 1.8	67.15 ± 1.07	7.19 ± 0.46	7.91 ± 0.69	N/A

Table 6 Percentage changes in mechanical responses compared to the vertical direction with bolded values showing no statistical difference between samples

Orientation	UTS (%change)	Yield strength (%change)	Elastic modulus (% change)	Elongation (%change)	Area reduction (%change)	Room temperature impact energy (%change)
Vertical	N/A	N/A	N/A	N/A	N/A	N/A
Horizontal	-1.85	8.33	14.8	53.4	35.5	61.7
45°	-0.14	8.33	16.0	22.3	4.02	N/A

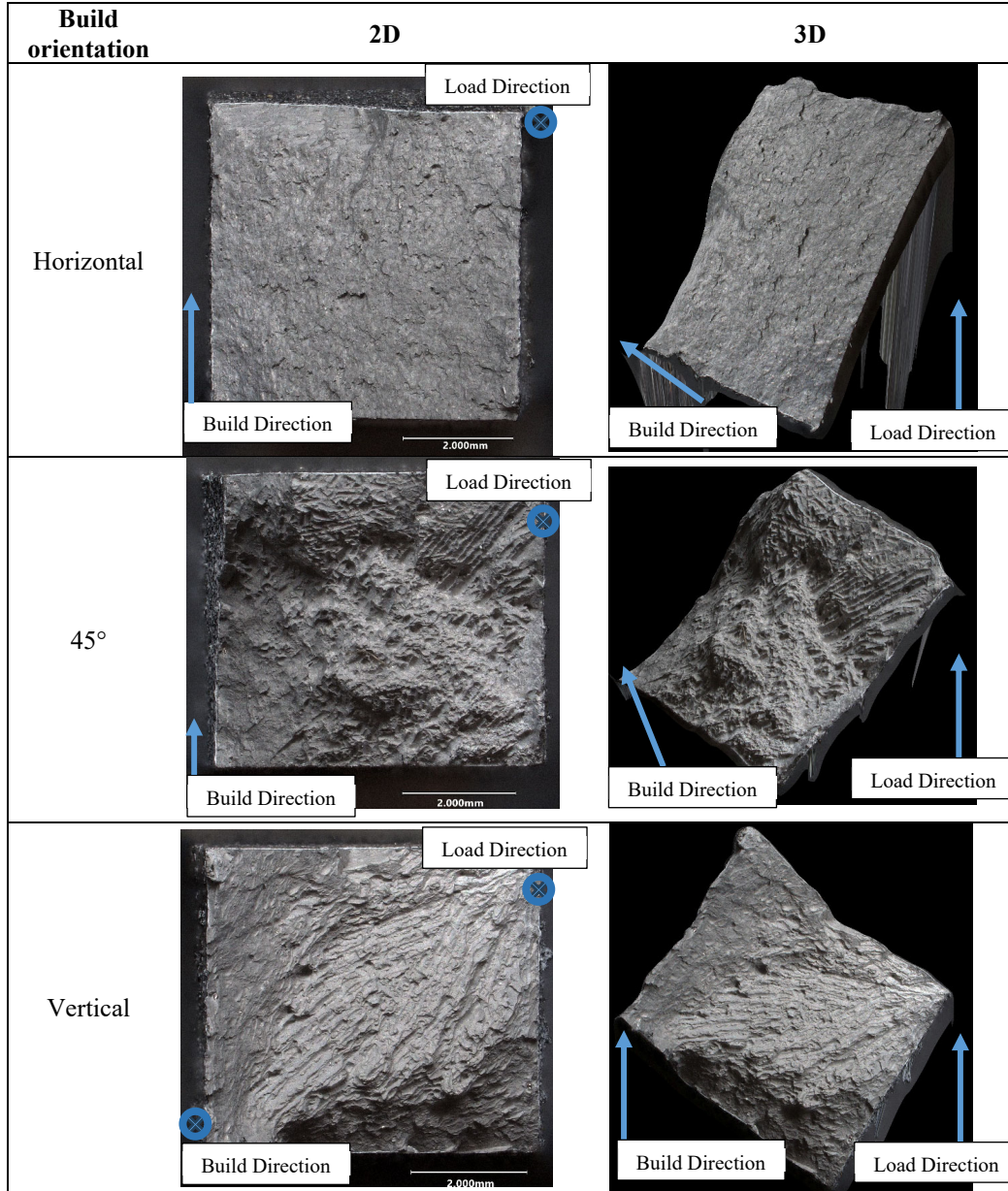


Fig. 4 2D and 3D micrographs of fracture surface of tensile samples

Although the horizontal samples showed a slight decrease in UTS, they outperformed the vertical samples in every other metric. Primarily, samples built in the horizontal direction displayed much higher toughness and ductility, with slight increases in elastic modulus and yield strength. The fracture surfaces highlight the difference in failure modes.

The horizontal samples fractured in typical ductile fashion. The vertical samples show some evidence of ductile behavior, but this is dominated by a fracture surface perpendicular to the loading direction, which indicates brittle failure. These samples have visible melt pool pullout, the interfaces of which most likely served

as an initiation point for failure. The 45° samples still show evidence of melt pool pullout, but primarily they show ductile fracture, similar to the horizontal samples.

The only case in which the 45° samples were statistically different from both the horizontal and the vertical samples was in the strain to failure, in which its mean (7.19%) fell between the other two cases (H = 10.3%, V = 5.88%). For area reduction, the 45° samples were not statistically different from the horizontal or vertical sample; however, the horizontal and vertical samples were dissimilar to each other. In this case, for area reduction, the 45° direction can display performance similar to the horizontal or vertical samples. In all other cases, the 45° samples were statistically similar to the better performing samples. (For a more detailed representation of the mechanical testing results paired with ANOVA analysis relationships, see the Appendix.)

5. Conclusion

The effect of build orientation on LPBF additively manufactured (AM) AlSi10Mg alloy was quantified. It was found that the toughness and ductility greatly increased in the horizontal direction, with a minor but statistically significant decrease in UTS. The vertical and horizontal results were statistically different from each other in all cases. The samples printed at a 45° angle were either statistically similar to one or both or the other build directions, or their performance was dissimilar and fell between the vertical and horizontal samples.

The dependence of mechanical performance on build orientation in LPBF yields some design considerations. For critical components, researchers and engineers can make informed decisions regarding part orientation with respect to the loading directions of the part, especially in cases in which high toughness is required. This enables a higher confidence in fielded AM parts, and it opens the door for parts specifically used for anisotropic mechanical properties. Researchers should further investigate the cause of this anisotropy and how it can be used in a mission critical part.

6. References

1. ASTM E8. Standard test methods for tension testing of metallic materials. ASTM International; 2013.
2. ASTM E23. Standard test methods for notched bar impact testing of metallic materials. ASTM International; 2023.

Appendix. Mechanical Testing Results

This appendix contains supplemental graphs depicting the average measured mechanical properties. Figure A-1 depicts the tensile properties with respect to build orientation, and Fig. A-2 depicts impact toughness results. The graphs contain error bars representing the standard deviation of each data set and tie lines connecting data sets that were found to be statistically similar.

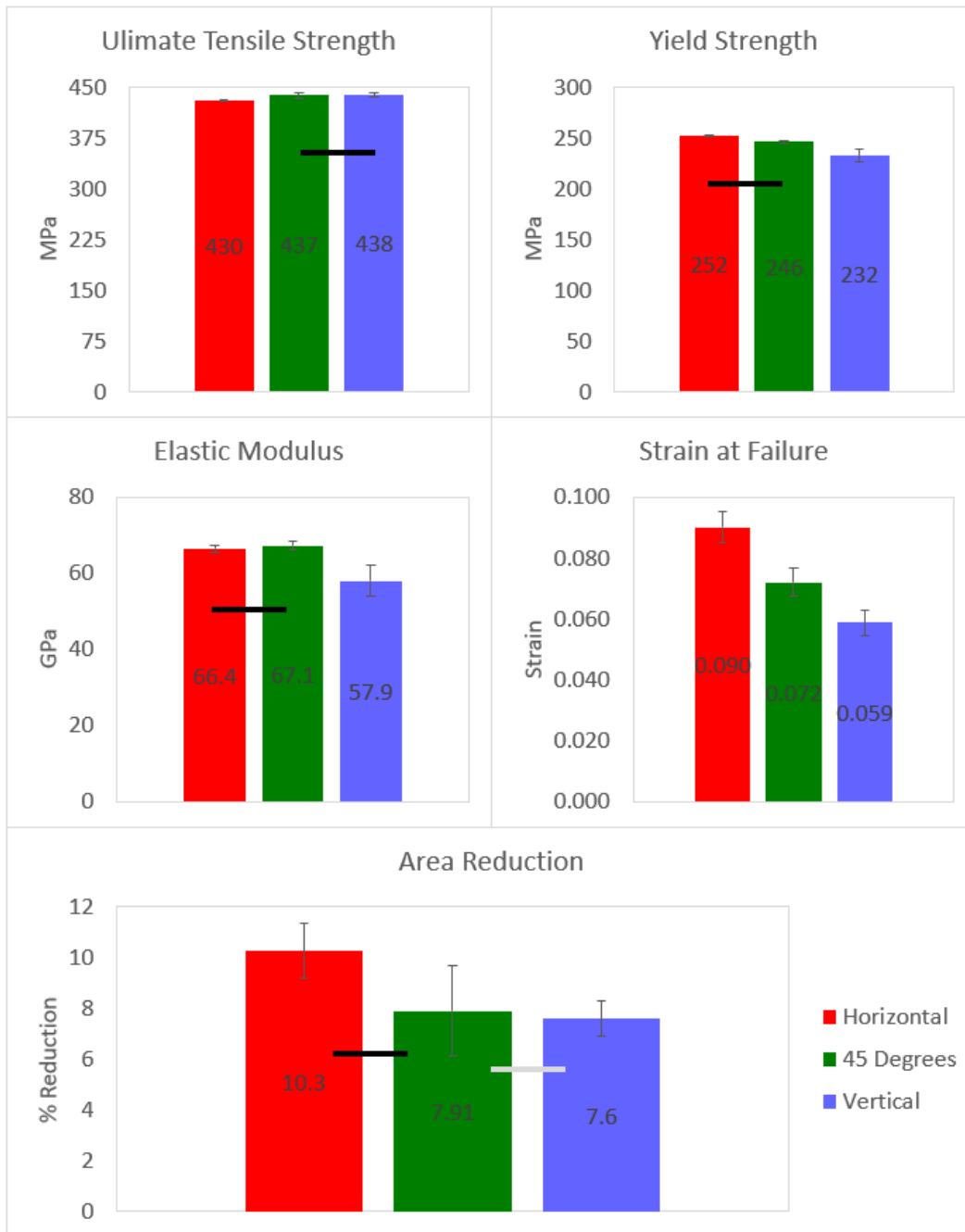


Fig. A-1 Tensile testing results with lines denoting which samples were statistically similar

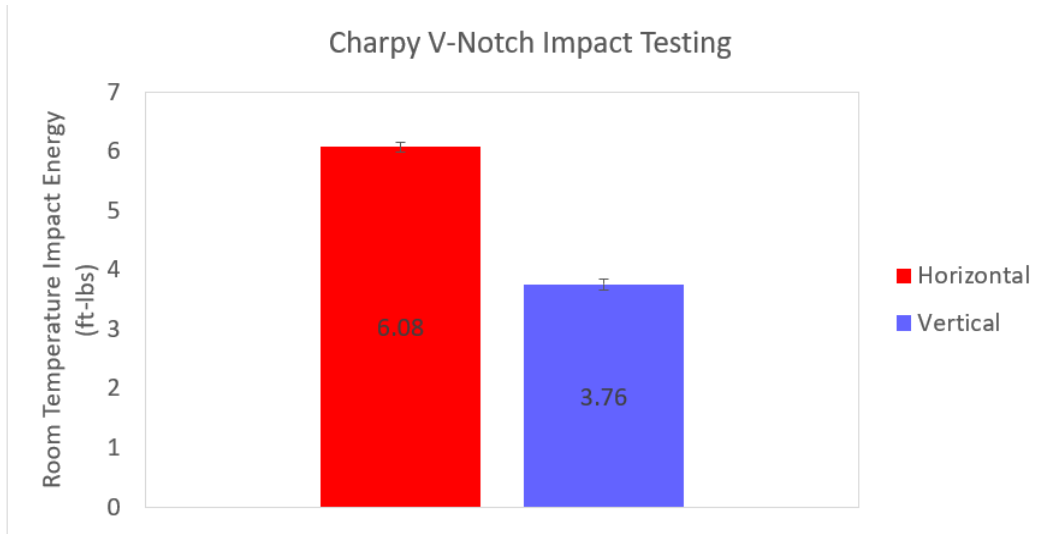


Fig. A-2 Impact testing results

List of Symbols, Abbreviations, and Acronyms

2D/3D	two-/three-dimensional
AlSi10Mg	aluminum, silicon, magnesium alloy
AM	additively manufactured
ANOVA	analysis of variance
df	degrees of freedom
LPBF	laser-powder bed fusion
MS	mean squares
N/A	not applicable
OEM	Original Equipment Manufacturer
SS	sum of squares
UTS	ultimate tensile strength